Frequency upconversion in a Pr3+ doped chalcogenide glass containing silver nanoparticles

Vineet Kumar Rai, Cid B. de Araujo, Yannick Ledemi, Bruno Bureau, Marcel Poulain, Xianghua Zhang, Y. Messaddeq

Frequency upconversion in a Pr^{3+} doped chalcogenide glass containing silver nanoparticles

Vineet Kumar Rai,[1] Cid B. de Araújo,[1,a)] Y. Ledemi,[2] B. Bureau,[2] M. Poulain,[2] X. H. Zhang,[2] and Y. Messaddeq[3]
[1]*Departamento de Física, Universidade Federal de Pernambuco, 50670-901 Recife, Pernambuco, Brazil*
[2]*UMR 6226 Sciences Chimiques de Rennes-Equipe Verres et Céramiques, Université de Rennes 1, 35042 Rennes, France*
[3]*Laboratorio dos Materiais Fotônicos, Instituto de Química, Universidade Estadual Paulista-UNESP, 14800-900 Araraquara, São Paulo, Brazil*

(Received 6 December 2007; accepted 18 March 2008; published online 23 May 2008)

We report on orange-to-blue frequency upconversion (UC) in Pr^{3+} doped chalcogenide glass ($Ga_{10}Ge_{25}S_{65}$) doped with Ag_2S and heat treated under different conditions to nucleate silver nanoparticles (NPs). The experiments were performed using 7 ns pulses from a dye laser that operates at ~590 nm, in resonance with the $^3H_4 \rightarrow {}^1D_2$ transition of Pr^{3+} ions. The enhancement observed in the UC emission at ~494 nm, ascribed as $^3P_0 \rightarrow {}^3H_4$ transition of the Pr^{3+} ion, is attributed to the large local field acting on the emitting ions due to the presence of the metallic NPs.
 [DOI: 10.1063/1.2927402]

I. INTRODUCTION

Rare earth ion (REI) doped materials are of great importance due to their wide range of applications in lasers, optical amplifiers, and optical sensors, among other devices.[1–4] Materials that present large potential for such uses are glasses having low cutoff phonon energy. For those materials, it is observed that the luminescence intensity of REI introduced as doping is enhanced several fold.[5–12] Usually, in order to make devices with optimized photonic properties, the REI concentration needs to be kept low to minimize luminescence quenching.[13] However, an alternative way to compensate the deleterious effect of quenching is to modify the REI environment.[14]

The introduction of metallic nanoparticles (NPs) in REI doped glasses have been exploited to enhance the luminescence efficiency provided that the wavelength of the excitation beam or the luminescence is near to the surface plasmon resonance (SPR) wavelength.[15] For instance, enhancement of Eu^{3+} luminescence was reported in a fluoroborate glass containing silver NPs a long time ago.[16] Later, experiments were presented where local field or energy transfer effects change the luminescence of REI in fluoroborate and silicate glasses.[17,18] Presently, this approach to increase the luminescence in REI doped glass is receiving renewed attention due to the large interest in nanophotonics. Accordingly, luminescence enhancement due to the presence of metallic NPs has been reported for Pr^{3+} and Er^{3+} in oxide glasses (see, for example, Refs. 19 and 20), but there are not many examples of other glasses being investigated through this approach.

Among the technologically important glasses available, the chalcogenide glasses (based on chalcogen elements: S, Se, and Te generally mixed with elements such as Ge, Ga, Sb, As, etc.) are important candidates for studies of luminescence enhancement by the influence of surface plasmons. These glasses are known for their low cutoff phonon energy (~350 cm^{-1}), extended infrared transparency, high refractive index, and large nonlinear optical properties. Recently, chalcohalide glass-ceramics with enhanced optical and mechanical properties have been synthesized both for passive applications (multispectral imaging)[21] and active applications for rare earth doping.[22] Glasses based on the (Ga_2S_3)–(GeS_2) system have been largely studied for their high photosensitivity,[23] high REI solubility, and large transparency in the visible range, as compared to other chalcogenide glass systems.[24,25] One example of this class of materials is the $Ga_{10}Ge_{25}S_{65}$ (GGS) glass, which presents very good chemical durability and thermal stability, high refractive index ($n \sim 2.2$ at 632.8 nm), and a transmittance window extending from the visible range to the infrared (0.46–12 μm).

The present paper envisages orange-to-blue frequency upconversion (UC) process in Pr^{3+} doped GGS containing Ag_2S, heat treated to nucleate silver NPs. The goal of the present work is to investigate the influence of NPs on the UC process to the blue region, which is excited using orange light from a dye laser pumped with the second harmonic of a Nd:YAG (yttrium aluminum garnet) laser. The contribution of the SPR associated with the NPs is demonstrated through the enhancement of the blue light intensity generated due to the UC process.

II. EXPERIMENTAL DETAILS

The glassy samples were prepared by the classical melt-quenching method. Two Pr^{3+} doped compositions were prepared for this study: $(Ga_{10}Ge_{25}S_{65})_{99.75}$–$Pr_{0.25}$ and $(Ga_{10}Ge_{25}S_{65})_{99.25}$–$Pr_{0.25}$–$(Ag_2S)_{0.5}$ labeled as GGSPr and GGSAgPr, respectively. A Pr^{3+} free composition $(Ga_{10}Ge_{25}S_{65})_{99.5}$–$(Ag_2S)_{0.5}$, labeled GGSAg, was also prepared in order to compare the NPs nucleation ability to that of the GGSAgPr samples.

High purity polycrystalline germanium (5N), gallium (5N), sulfur (5N), and Pr (4N) were used for the synthesis while silver was added in the form of sulfide (Ag_2S, 5N). The elements were weighed to prepare 10 g of glass and

a)Author to whom correspondence should be addressed. Electronic mail: cid@df.ufpe.br.

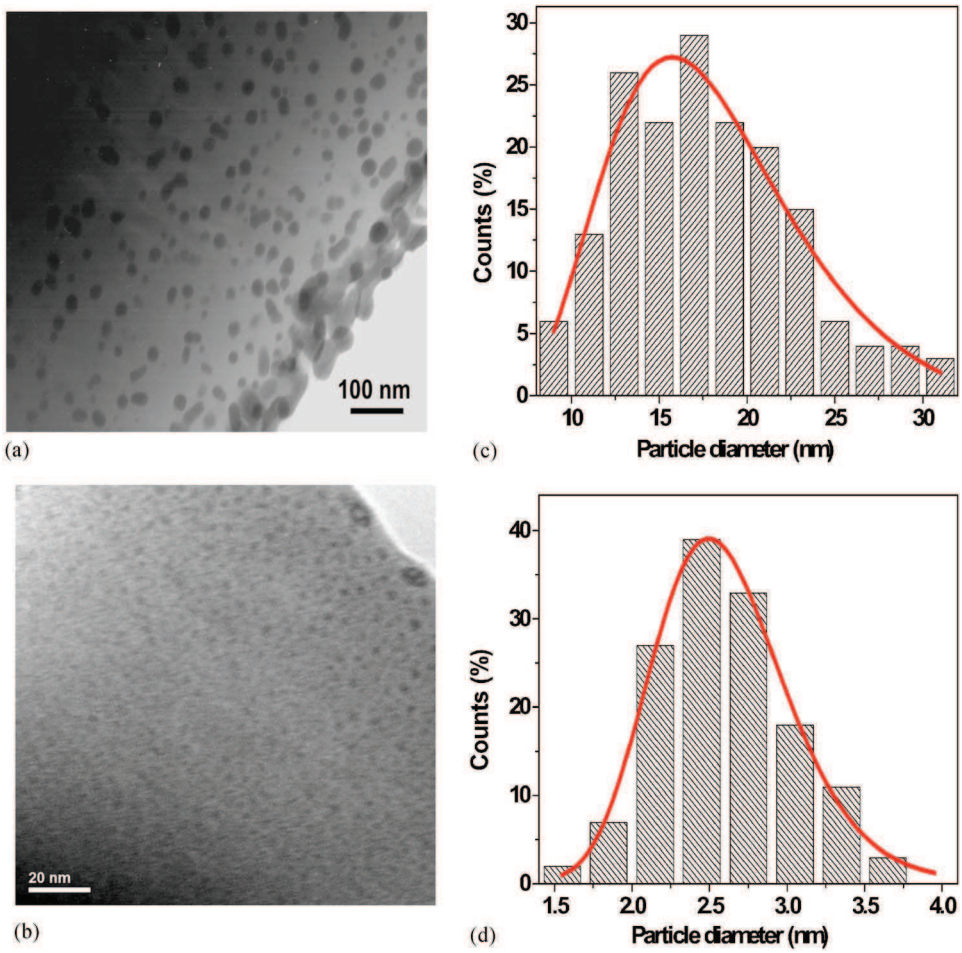

FIG. 1. (Color online) TEM images for samples annealed during 23 h: (a) GGSAg and (b) GGSAgPr. The respective nanoparticles size distributions are presented in (c) and (d). The solid lines represent log-normal distribution functions fitted to the histograms.

introduced into a silica tube (9 mm inner diameter); a vacuum of about 10^{-4} mbar was achieved in the tube before being sealed. The ampoule was then introduced in a rocking tubular furnace and slowly heated up to 900 °C in order to allow thorough reaction of the starting compounds and to avoid explosion due to the sulfide high vapor pressure. The batch was homogenized during 8 h at this temperature, then the rocking was stopped, and the ampoule kept in vertical position during 20 min to reduce the formation of bubbles in the glass. The ampoule was taken out from the oven, quenched in water at room temperature, annealed at 370 °C during 3 h and, finally, slowly cooled down to ambient temperature in order to reduce the internal stress caused by the quenching. Then, the silica ampoule was opened and the obtained glass rod was removed, cut, and polished. All samples were prepared following this procedure.

The characteristic temperatures of the obtained glasses were measured by using a differential scanning calorimeter from room temperature to 550 °C with a heating rate of 10 °C/min. The three glasses present a glass transition temperature $T_g \approx 426$ °C and an onset crystallization temperature $T_x \approx 540$ °C.

The samples were then submitted to heat treatment at 370 °C for 20 and 30 h in the ambient atmosphere to thermally reduce the Ag^+ ions into Ag^0 and to nucleate metallic NPs. Thus, in fact, the glasses were heat treated at 370 °C for 3 h (corresponding to the necessary annealing during the glass synthesis), 23, and 33 h. For a better readability, the heat-treated samples are named GGSPr-*t* and GGSAgPr-*t* with *t* being the heat-treatment time (t=3, 23, and 33 h). Crystallization of the glassy matrix did not occur because the heat-treatment temperature was below T_g.

An ~200 kV transmission electron microscope (TEM) equipped with an energy dispersive spectroscopy probe was used to observe the NPs. All the samples were uniformly thinned by ion milling for these imaging experiments.

For the luminescence experiments, a Nd:YAG laser pumped dye laser (wavelength: ~590 nm; pulses of 7 ns at a repetition rate of 5 Hz; peak power of ~20 kW; linewidth of ~0.5 cm^{-1}) was used. The linearly polarized excitation beam was focused onto the bulk sample with a lens of 5 cm focal length and the fluorescence was collected in a direction perpendicular to the incident beam. The signal was analyzed by a 0.5 m spectrophotometer (with resolution of 0.5 nm) attached with a GaAs photomultiplier. The signals were recorded using a digital oscilloscope connected to a computer. All measurements were made at room temperature.

III. RESULTS AND DISCUSSIONS

Figures 1(a) and 1(b) illustrate the behavior of the samples showing TEM images of GGSAg-23 and GGSAgPr-

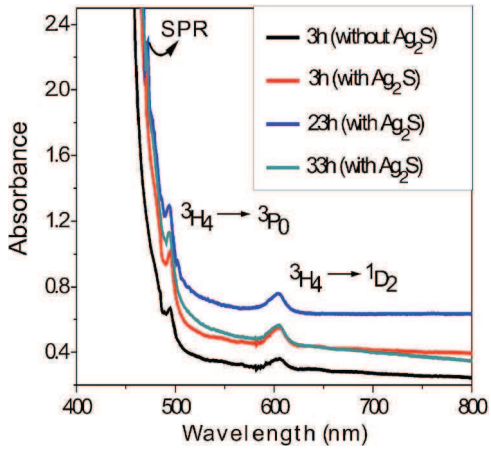

FIG. 2. (Color online) Absorbance spectra of the GGSPr sample (with and without metallic nanoparticles) for different annealing times as indicated in the legend. Sample thickness: 3.9 mm.

23. The average size of the metallic NPs was found to decrease in the presence of the Pr^{3+} ions. This effect is attributed to the possibility of competing reduction processes involving Ag^{+} and Pr^{3+}. The average diameter of the NPs was determined assuming log-normal distributions, as indicated by the lines in Figs. 1(c) and 1(d). Therefore, the average diameter of the NPs in the sample without Pr^{3+}, submitted to 23 h of annealing time, is 18 ± 1 nm; in the presence of the Pr^{3+} ions, it is reduced to 2.6 ± 0.1 nm for the same heat-treatment time.

Figure 2 shows the absorbance spectra of the samples annealed for different times. Bands associated with Pr^{3+} transitions from the ground state ($^3H_4$) to excited states[1] and a feature at ~472 nm attributed to SPR of the NPs are observed. The SPR wavelength (λ_{SP}) calculated using Mie theory,[15] considering spherical particles, the dielectric function of bulk silver,[26] and the glass refractive index, is ≈485 nm. This result represents a reasonable agreement with the experimental value since the effect of the metal-glass interface is not considered in the calculations neither the NP's shape. The amplitude of the band at ~472 nm increases while increasing the concentration of the NPs which grows up for heat-treatment time of 23 h. For a heat-treatment time longer than 23 h, a reverse trend is observed for the concentration. No shift of the band peaking at ~472 nm was observed for different annealing times.

Figure 3 shows the luminescence spectra of GGSPr-23 and GGSAgPr-23. Two bands are observed peaking at ~494 and at ~680 nm ascribed as $^3P_0 \rightarrow {}^3H_4$ and $^1D_2 \rightarrow {}^3H_5$ transitions, respectively. The intensity of the UC signal depends quadratically with the laser intensity indicating that two laser photons are absorbed to produce one photon corresponding to the $^3P_0 \rightarrow {}^3H_4$ transition. On the other hand, the intensity of the $^1D_2 \rightarrow {}^3H_5$ transition (Stokes emission) depends linearly with the laser intensity. It is important to notice that the ratio between the integrated UC and Stokes signals is larger for the sample with metallic NPs.

A simplified energy level diagram for the Pr^{3+} ions is shown in Fig. 4 with indication of the radiative transitions studied here, as well as the location of the SPR band.

The UC emission reported here has been recently inves-

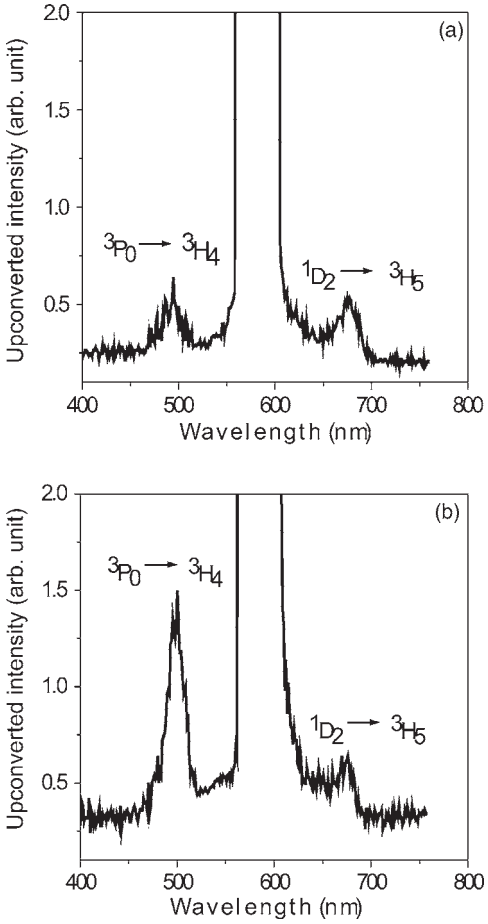

FIG. 3. Luminescence spectra for the samples heat treated during 23 h (excitation wavelength: 590 nm): (a) GGSPr and (b) GGSAgPr. The strong signal centered at 590 nm is due to the scattered laser beam.

tigated in Pr^{3+} doped tellurite glasses[27] but in the absence of metallic NPs. In that case, the blue signal originates from an energy transfer (ET) process that involves pairs of Pr^{3+}. Two ions in the $^1D_2$ level exchange energy in such way that one ion is promoted to the $[^3P_J(J=0,1,2), {}^1I_6]$ manifold and the other decays to lower energy levels. Afterward, the blue luminescence is produced due to transition $^3P_0 \rightarrow {}^3H_4$. Due to the ET process, the UC signal shows a rise time larger than the laser pulse duration and a decay time of the order of the $^1D_2$ lifetime ($\approx 10^2$ μs). In the present case, the temporal evolution of the UC luminescence is in accord with the mechanism of ET involving pairs of Pr^{3+} ions, as in Ref. 27.

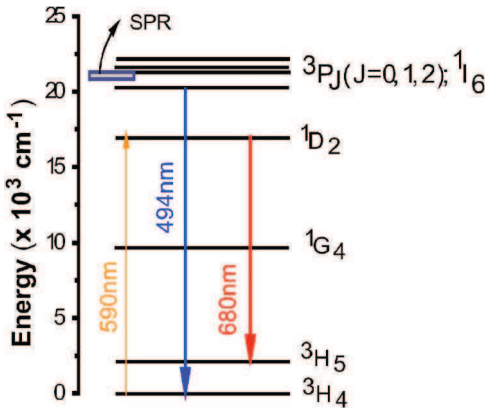

FIG. 4. (Color online) Simplified energy level diagram for Pr^{3+} ions.

TABLE I. The ratio between the integrated intensities of $^3P_0 \rightarrow {}^3H_4$ and $^1D_2 \rightarrow {}^3H_5$ emission bands for samples heat treated during different times.

Sample	Heat-treatment time (h)	Ratio ($^3P_0 \rightarrow {}^3H_4/{}^1D_2 \rightarrow {}^3H_5$)
GGSPr-3	3	0.98
GGSAgPr-3	3	1.10
GGSAgPr-23	23	2.30
GGSAgPr-33	33	0.96

It is important to notice that although enhancement of the UC emission intensity has been observed in the presence of the metallic NPs (GGSAgPr-23 sample), negligible difference in the intensity of the band associated with the $^1D_2 \rightarrow {}^3H_5$ transition (with and without NPs) was observed. On the other hand, the UC spectra of the GGSPr glass without silver, heat treated for different times, show no change indicating that the presence of NPs is essential to obtain enhanced emission. Moreover, no evidence of change in the glass structure neither nucleation of NPs due to the influence of the laser was observed. This is understood considering that the laser pulses have low energy and the pulses repetition rate is small.

We recall that photoinduced effects (such as photodarkening, photobleaching, and photoexpansion) may be observed in the glass composition studied here.[23] However, those effects are relevant when the samples are exposed to continuous wave UV light for long time intervals. In the present case, no such photoinduced effect was observed.

The heat-treatment influence on the ratio between the integrated intensities of $^3P_0 \rightarrow {}^3H_4$ and $^1D_2 \rightarrow {}^3H_5$ transitions is summarized in Table I. Notice that the ratio increased by more than ~100% for the sample with silver that was heat treated during 23 h. This is due to the local field around the NPs that is strongly enhanced by the contribution of the surface plasmons. Clearly, the results show that the UC signal, which corresponds to a wavelength near from λ_{SP}, is more affected by the NPs than the emission from the $^1D_2$ level which has a larger detuning from the SPR than the $[^3P_J (J=0,1,2), {}^1I_6]$ manifold. The smaller ratio corresponding to GGSAgPr-33 sample is not well understood at the present time. Of course, the reduction in the NP's concentration, which corresponds to a decrease in the SPR amplitude, may contributes to the decrease in the ratio of intensities. However, the possibility of quenching of the blue emission due to the smaller average distances between the Pr^{3+} ions and the NPs may also give origin to reduction in the blue intensity since ET from the Pr^{3+} ions to the NPs may become efficient. The understanding of the phenomena involved in this case requires further work beyond the scope of the present paper.

IV. SUMMARY

In summary, we reported the synthesis of Pr^{3+} doped chalcogenide glass containing silver NPs and investigate their luminescence properties. The excitation was in resonance with the $^3H_4 \rightarrow {}^1D_2$ transition that occurs in the orange spectrum (~590 nm). Enhancement of the frequency UC process that leads to emission at 494 nm was observed due to the presence of the metallic NPs. This observation corroborates the expectation of the enhanced local field effect on the ions located in the proximity of the NPs. On the other hand, quenching was also observed for samples heat treated for longer times, which indicates that ET occurs from the Pr^{3+} ions to the metallic NPs. This result is important in the sense that it demonstrates that there is an optimum heat-treatment time of samples to observe enhanced frequency UC due to nucleation of metallic NPs.

ACKNOWLEDGMENTS

The authors acknowledge financial support from the Brazilian agencies Conselho Nacional de Desenvolvimento Científico e Tecnológico (CNPq), Fundação de Amparo à Ciência e Tecnologia de Pernambuco (FACEPE), and the CAPES-COFECUB project (Contract No. 471/04). This work was performed under the Nanophotonics Network Project and Millenium Institute on Nonlinear Optics, Photonics and Bio-Photonics. We also acknowledge Dr. J. Dexpert-Ghys (CEMES-Toulouse-France).

[1] *Rare Earth Doped Fiber Lasers and Amplifiers*, edited by M. J. F. Digonnet (Dekker, New York, 1993).
[2] J. A. Savage, Mater. Sci. Rep. **2**, 99 (1987).
[3] S. D. Jackson, Appl. Phys. Lett. **83**, 1316 (2003).
[4] V. K. Rai, Appl. Phys. B: Lasers Opt. **88**, 297 (2007).
[5] A. J. Kenyon, Prog. Quantum Electron. **26**, 225 (2002).
[6] L. F. Johnson and H. J. Guggenheim, Appl. Phys. Lett. **19**, 44 (1971).
[7] G. Poirier, F. C. Cassanjes, C. B. de Araújo, V. A. Jerez, S. J. L. Ribeiro, Y. Messaddeq, and M. Poulain, J. Appl. Phys. **93**, 3259 (2003).
[8] R. El-Mallawany, A. Patra, C. S. Friend, R. Kapoor, and P. N. Prasad, Opt. Mater. (Amsterdam, Neth.) **26**, 267 (2004).
[9] G. S. Murugan, T. Susuki, and Y. Ohishi, Appl. Phys. Lett. **86**, 161109 (2005).
[10] C. B. de Araújo, L. R. P. Kassab, R. A. Kobayashi, L. P. Naranjo, and P. A. S. Cruz, J. Appl. Phys. **99**, 123522 (2006).
[11] V. K. Rai, K. Kumar, and S. B. Rai, Opt. Mater. (Amsterdam, Neth.) **29**, 873 (2007).
[12] G. Poirier, V. A. Jerez, C. B. de Araújo, Y. Messaddeq, S. J. L. Ribeiro, and M. Poulain, J. Appl. Phys. **93**, 1493 (2003).
[13] E. Snoeks, P. G. Kik, and A. Polman, Opt. Mater. **5**, 159 (1996).
[14] E. Snoeks, A. Lagendijk, and A. Polman, Phys. Rev. B **74**, 002459 (1995).
[15] P. N. Prasad, *Nanophotonics* (Wiley, New York, 2004).
[16] O. L. Malta, P. A. S. Cruz, G. F. da Sá, and F. Auzel, J. Lumin. **33**, 261 (1985).
[17] O. L. Malta and M. A. C. dos Santos, Chem. Phys. Lett. **174**, 1513 (1999).
[18] T. Hayakawa, S. T. Selvan, and M. Nogami, Appl. Phys. Lett. **74**, 1513 (1999).
[19] L. P. Naranjo, C. B. de Araújo, O. L. Malta, P. A. S. Cruz, and L. R. P. Kassab, Appl. Phys. Lett. **87**, 241914 (2005).
[20] D. M. da Silva, L. R. Pires Kassab, S. R. Luthi, C. B. de Araújo, A. S. L. Gomes, and M. J. V. Bell, Appl. Phys. Lett. **90**, 081913 (2007).
[21] L. Calvez, H. L. Ma, J. Lucas, and X. H. Zhang, Adv. Mater. (Weinheim, Ger.) **19**, 129 (2007).
[22] V. Seznec, H. L. Ma, X. H. Zhang, V. Nazabal, J. L. Adam, X. S. Qiao, and X. P. Fan, Opt. Mater. (Amsterdam, Neth.) **29**, 371 (2006).
[23] S. H. Messaddeq, V. R. Mastelaro, M. S. Li, M. Tabackniks, D. Lezal, A. Ramos, and Y. Messaddeq, Appl. Surf. Sci. **205**, 143 (2003).
[24] R. Balda, A. Mendioroz, J. Fernández, M. A. Arriandiaga, L. S. Griscom, and J. L. Adam, Opt. Mater. (Amsterdam, Neth.) **16**, 249 (2001).
[25] L. Petit, N. Carlie, K. Richardson, A. Humeau, S. Cherukulappurath, and G. Boudebs, Opt. Lett. **31**, 1495 (2006) and references therein.
[26] E. D. Palik, *Handbook of Optical Constants of Solids* (Academic, New York, 1985).
[27] V. K. Rai, L. de S. Menezes, and C. B. de Araújo, J. Appl. Phys. **101**, 123514 (2007).